Environmental Science & Technology

pubs.acs.org/est

Article

Chlorination (but Not UV Disinfection) Generates Cell Debris that Increases Extracellular Antibiotic Resistance Gene Transfer via Proximal Adsorption to Recipients and Upregulated Transformation Genes

Qingbin Yuan, Pingfeng Yu,* Yuan Cheng, Pengxiao Zuo, Yisi Xu, Yuxiao Cui, Yi Luo, and Pedro J. J. Alvarez*

Cite This: *Environ. Sci. Technol.* 2022, 56, 17166–17176

Read Online

ACCESS | Metrics & More | Article Recommendations | Supporting Information

ABSTRACT: To advance the understanding of antibiotic resistance propagation from wastewater treatment plants, it is important to elucidate how different effluent disinfection processes affect the dissemination of predominantly extracellular antibiotic resistance genes (eARGs). Here, we show that, by facilitating proximal adsorption to recipient cells, bacterial debris generated by chlorination (but not by UV irradiation) increases the natural transformation frequency of their adsorbed eARG by 2.9 to 7.2-fold relative to free eARGs. This is because chlorination increases the bacterial surface roughness by 1.1 to 6.7-fold and the affinity toward eARGs by 1.6 to 5.8-fold, and 98% of the total eARGs released after chlorination were adsorbed to cell debris. In contrast, UV irradiation released predominantly free eARGs with 18% to 56% lower transformation frequency. The collision theory indicates that the ARG donor−recipient collision frequency increased by 35.1-fold for eARGs adsorbed onto chlorination-generated bacterial debris, and the xDLVO model infers a 29% lower donor−recipient contact energy barrier for these ARGs. Exposure to chlorination-generated bacterial debris also upregulated genes associated with natural transformation in *Vibrio vulnificus* (e.g., *tfoX* encoding the major activator of natural transformation) by 2.6 to 5.2-fold, likely due to the generation of chlorinated molecules (5.1-fold higher Cl content after chlorination) and persistent reactive species (e.g., carbon-centered radicals) on bacterial debris. Increased proximal eARG adsorption to bacterial debris was also observed in the secondary effluent after chlorination; this decreased eARG decay by 64% and increased the relative abundance of ARGs by 7.2-fold. Overall, this study highlights that different disinfection approaches can result in different physical states of eARGs that affect their resulting dissemination potential via transformation.

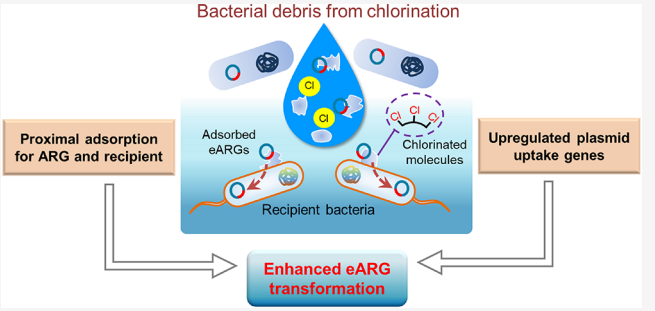

KEYWORDS: *chlorination, extracellular ARG, transformation, cell debris, proximal adsorption*

INTRODUCTION

The spread of antibiotic resistance is a global health concern linked to 4.95 million deaths in 2019.[1] Therefore, it is important to advance our understanding of the fate of antibiotic resistance genes (ARGs) in wastewater treatment plants (WWTPs), which are terminal collection points for antibiotics and ARGs and can be breeding grounds and point sources for discharging ARGs to the environment.[2,3] Notably, extracellular ARGs (eARGs) are commonly present during and after wastewater treatment processes, particularly effluent disinfection. Up to 10^{17}−10^{18} copies/day (or 10^{6}−10^{8} copies/L) of eARGs could be released from WWTPs, making eARGs the dominant form of ARGs discharged to the environment.[4,5] These eARGs may transform bacteria in receiving aquatic systems (e.g., river sediments[6]), which would augment the environmental resistome and associated public health risks.[7]

Chlorination and ultraviolet (UV) irradiation are the most common secondary effluent disinfection processes in most countries.[8] Both approaches are generally efficient for killing bacteria but not for removing ARGs since intracellular ARGs (iARGs) are mainly released as eARGs into the environment rather than destroyed after cell lysis.[3] Furthermore, disinfection generates bacterial debris from cell lysis[4,9] that free eARGs may adsorb to, forming adsorbed eARGs.[4] Previous studies showed that microplastic-adsorbed eARGs could have a higher

Received: August 24, 2022
Revised: October 12, 2022
Accepted: October 17, 2022
Published: October 26, 2022

transmission potential than free eARGs by facilitating proximal eARG−recipient adsorption.[10] However, little is known about the influence of different disinfection strategies and associated byproducts, specifically bacterial debris, on eARG physical states (e.g., free or adsorbed ARG) and their dissemination potential.

Chlorination can generate oxidized bacterial debris with altered affinities for eARGs due to changes in the surface charge and hydrophobicity[11] caused by the chlorinated lipids and amino acids.[12] In contrast, UV irradiation kills bacteria mainly by destroying DNA[13] without substantially affecting the cell integrity. Disinfection by chlorination can also generate environmentally persistent reactive oxidative species (e.g., chlorinated radicals)[14] or chlorinated organics[15] that could influence the susceptibility of some bacteria to transformation by eARGs.[16] Thus, different disinfection methods produce bacterial debris with distinct properties that may interact with eARGs differently and have consequences on eARG persistence and transmissivity.

This study compares the effects of chlorination versus UV irradiation on WWTP effluent in terms of eARG abundance, transformation, and persistence. *E. coli* with a bla_{NDM-1} multidrug resistance gene (coding metallo-β-lactamase) was used as a model multidrug-resistant enteric bacterium. The importance of eARG adsorption onto cell debris for enhanced transformation was assessed separately using the competent reference strain *E. coli* HB101 or the natural competent strain *Vibrio vulnificus* (*V. vulnificus*) as the recipient. Notably, *V. vulnificus* is an important opportunistic human pathogen frequently detected in wastewater, freshwater, and marine environments.[17−19] Changes in the affinity of cell debris for eARG caused by chlorination were examined by atomic force microscopy (AFM) and extended Derjaguin−Landau−Verwey−Overbeek (xDLVO) theory. We also quantified how attachment to cell debris affects the expression of genes regulating the natural transformation of *V. vulnificus*, which could be affected by chlorinated byproducts.[20] Overall, this study demonstrates that different wastewater effluent disinfection strategies may affect the potential for a horizontal transfer of ARGs via transformation.

MATERIALS AND METHODS

Chemicals, Bacterial Strains, and Plasmids. NaClO (5%), Na_2SO_3 (≥98%), isoamyl acetate (≥99%), glutaraldehyde (25% in H_2O), and KBr (≥99%) were purchased from Sigma-Aldrich (United States) and used as received. Kanamycin sulfate (USP grade), chitin (bio grade), and colistin sulfate (bio grade) were purchased from Aladdin (Shanghai, China). Plasmid PET29 with multidrug resistance gene bla_{NDM-1} was used for natural transformation,[21] while *V. vulnificus* (accession no. CP046835.1) served as the recipient. Plasmid PET29 was incorporated into commercial competent strain *E. coli* HB101 and cultivated in Luria Broth medium with 50 μg/mL ampicillin and 50 μg/mL kanamycin. Overnight cultured *E. coli* HB101 harboring plasmid PET29 was collected with centrifugation and then washed with phosphate-buffered saline (PBS) three times. The bacteria were resuspended in PBS to 0.8 optical density at 600 nm (OD_{600}) prior to use. Municipal wastewater samples were collected from the secondary effluent of a wastewater treatment plant located in Nanjing, China (see Table S1 for physical and chemical parameters).

ARB and ARG Disinfection. For disinfection with chlorination, NaClO solution (1.0 g/L) was spiked into 40 mL of *E. coli* suspensions (~10^8 CFU/mL) with final concentrations of active chlorine at 0.5, 1.0, 3.0, and 5.0 mg/L.[22] The mixtures were then stirred at 300 rpm for 10 min at room temperature before termination with $Na_2S_2O_3$ (1.0 g/L). The above chlorination dosages referred to 5, 10, 30, and 50 mg (active Cl) min/L. For disinfection with UV irradiation, Petri dishes containing 40 mL of the *E. coli* suspension were irradiated under a low-pressure mercury UV lamp (120 W, TL120W/01, Philips) for 10 min with stirring at 320 rpm. Various UV fluences (5, 10, 50, and 100 mJ/cm^2) were achieved by adjusting the distance between the Petri dishes and UV lamp.[23]

The wastewater secondary effluent (characterized in Table S1) was also processed by chlorination and UV irradiation following the above procedures. Considering the potential interference by competing pollutants in wastewater, larger chlorine doses (i.e., 10, 50, 100, and 500 mg min/L) or UV fluences (50, 100, 200, and 400 mJ/cm^2) were adopted, which were within commonly used levels in water treatment processes.[9] Different forms of the bacterial genome (i.e., iDNA, free eDNA, and adsorbed eDNA) were extracted from samples before and after disinfection as described below.

iDNA and eDNA Extraction and Quantification. The extraction of iDNA, free eDNA, and adsorbed eDNA was processed as previously described.[5] Briefly, 10 mL of the disinfection mixture was centrifugated for 5 min (10,000 × *g*) and then filtered through a 0.22 μm membrane to completely separate a-eDNA (and iDNA) from the solution. The filtrate was collected for f-eDNA extraction by magnetic beads, while the pellet and membrane were immersed in 10 mL of PBS with continuous shaking at 250 rpm for 10 min followed by filtration thorough another 0.22 μm membrane. The acquired filtrate was collected for adsorbed eDNA extraction using magnetic beads, while the two membrane filters were collected for iDNA extraction using a Fast DNA SPIN kit for soil (MPbio, USA) according to the manufacturer's instructions. The details of eDNA extraction using magnetic beads are available in the Supporting Information (Text S1).

The abundance of the bla_{NDM-1} gene in the *E. coli* disinfection experiment, and *tetA* in the wastewater effluent disinfection experiment were quantified by qPCR, with details presented in Text S2 and Table S2. The released eDNA post disinfection was visualized by confocal microscopy. Briefly, 10 μL of the bacterial suspension post disinfection was placed onto a sterilized glass slide and spiked with 5 μL of 10,000× Gel-green (Beyotime Biotechnology, China) followed by gently mixing. After incubation for 20 min, stained samples were observed by confocal microscopy (ZEISS LSM 900 with Airyscan 2, Germany). The excitation and emission wavelength (E_x/E_m) were set at 497 and 540 nm, respectively.

Characterization of Bacterial Debris after Disinfection. Bacterial morphology after disinfection was examined by scanning electron microscopy (SEM), transmission electron microscopy (TEM), and atomic force microscopy (AFM). Briefly, the bacterial suspension after disinfection was fixed with 3% (*v*/*v*) prechilled glutaraldehyde and then dehydrated in a series of ethanol−water solutions followed by further treatments of the ethanol and isoamyl acetate mixture (vol/vol = 1:1).[24] For SEM observation, the sample was sputter-coated with an ~7 nm gold film using a Denton Desk V Sputter System and then observed using an HITACHI SU8010 SEM.

https://doi.org/10.1021/acs.est.2c06158
Environ. Sci. Technol. 2022, 56, 17166−17176

For TEM observation, the sample was dropped onto a copper grid and observed after drying using a JEOL 2010F (Japan) at 200 kV. The morphology of the bacterial debris was further examined by an AFM (Park NX20, Parksystems, United States), and the roughness was acquired based on the image.

Bacterial surface oxidation was examined by Fourier transform infrared spectroscopy (Nicolet iS50 FTIR, Thermo Scientific, United States) and X-ray photoelectron spectroscopy (XPS) equipped with a 400 μm Al Kα ray (K-Alpha, Thermo Fisher, United States).[21] The pass energy was 100 eV for the survey and 50 eV for the high-resolution elemental analysis. The hydrophobicity of bacteria debris was determined by contact-angle measurements (Zhongchen JC2000C, China), while the zeta potential and size were determined using a Zeta Potential Analyzer (Zeta PALS, United States) with details illustrated in the Supporting Information (Text S3). Changes in the cell membrane fluidity post chlorination or UV irradiation were measured by using 4′-(trimethylammonium) diphenylhexatriene (TMA-DPH).[25] Changes in the organic chlorine content of bacterial debris after chlorination were measured as the chloride released post sample digestion.[26] Briefly, chlorinated samples were washed thoroughly to remove residual disinfectant and chloride ions and then digested with NaOH (1 M, 250 °C). The chloride concentrations in the filtered extract of both chlorinated and non-disinfected controls were measured via ion chromatography (ICS-1100, Thermo Scientific, United States). Electron paramagnetic resonance (EPR) measurements were then taken at room temperature using a Bruker EMX micro-6/1/P/L spectrometer (Karlsruhe, Germany) to detect any environmentally persistent free radicals (EPFRs) that could be generated during chlorination or UV irradiation.[27]

Assessment of eDNA-Bacteria Interfacial Interactions. Force−distance (F−D) measurements were conducted on an atomic force microscope (AFM, Park NX20, Parksystems, United States) to assess the interfacial force between eDNA and bacteria as previously reported.[10] Briefly, the AFM tip was functionalized with a PCR product of bla_{NDM-1} through a stable Au−thiol interaction. *E. coli* HB101 after different extents of disinfection was deposited on freshly cleaved mica. Typical F−D curves with the binding force and rupture force were generated, and the most probable rupture force was obtained.[28] The details of AFM tip modification and measurement are available in the Supporting Information (Texts S4 and S5).

The xDLVO theory was applied to calculate the total interaction energy between *E. coli* and released plasmid PET29 after chlorination or UV irradiation. The xDLVO theory was established as the sum of three kinds of interactions, including the attractive van der Waals interaction (V_{VDW}), the repulsive electrostatic double-layer interaction (V_{EDL}), and the Lewis acid−base interaction (V_{AB}).[29] Calculation details are available in Text S6.

The collision frequency among ARGs (f-eARG and a-eARG) and the recipient was estimated using collision theory[30] to determine the interaction frequency during transformation experiments. The collision theory has been previously used to assess the interaction frequency between DNA donors and recipients during a horizontal gene transfer.[31] The collision frequency is calculated using eq 1.

$$Z = \pi(r_1 + r_2)^2 u C_1 C_2 t \quad (1)$$

where Z is the collision frequency of ARGs and the recipient, and r_1 and r_2 are the radius of the DNA and recipient. For a-eARG, r_1 is the radius of bacterial debris. C_1 and C_2 are the concentrations of ARGs and the recipient during transformation. U is the relative velocity of ARGs and the recipient, which is approximated as the shaken speed (i.e., 10 r/min). t is the exposure period (4 h).

Transformation of eARGs into a Competent Reference Strain and Natural Competent Strain. The effect of the eARGs' physical state on transformation was assessed using reference strain *E. coli* HB101 as the recipient. Most eARGs were adsorbed to cell debris after chlorination or were free after UV irradiation. Thus, adsorbed and free eARGs were used as the donors to study transformation after chlorination or UV irradiation, respectively. For chlorination, free eARGs (plasmid PET29 with multidrug-resistance gene bla_{NDM-1}) were mixed with and adsorbed onto intact bacteria (*E. coli* HB101 without plasmids) or bacterial debris produced by chlorination at 5−50 mg min/L and treated as donors. For UV irradiation, free eARGs exposed to 50−400 mJ/cm^2 fluences were treated as donors. Details of these experiments are available in the Supporting Information (Text S7).

The natural transformation of eARGs was conducted using competent *V. vulnificus* as the recipient.[17,18,32,33] Briefly, the natural competence of *V. vulnificus* was prepared using a chitin-based assay.[17,18] Adsorbed eARGs (for chlorination) and free eARGs (for UV irradiation) were prepared as described above. The *V. vulnificus* suspension (~10^9 CFU/mL) was mixed with a-eARG or f-eARG and incubated statically at 30 °C for 24 h followed by incubation in fresh LB-N broth at 37 °C for 2 h. The transformants were enumerated by selective LB-N agar with kanamycin (50 μg/mL) and colistin (5 μg/mL). The presence of bla_{NDM-1} in transformants was verified by PCR followed by electrophoresis (Figure S1). The total number of *V. vulnificus* was counted by LB-N agar with colistin (5 μg/mL). Transformation frequencies were calculated as the ratio of the number of transformant CFUs to the total CFUs. The ROS production in *V. vulnificus* exposed to bacterial debris produced by chlorination or UV disinfection was investigated by measuring the fluorescence of DCF (dichlorodihydrofluorescein) using a DCF fluorescence kit (KeyGEN BioTECH, China).[34]

Transformation-Associated Gene Expression Analysis. Samples during natural transformation experiments were collected for transcriptomic analysis of six genes (i.e., *tfoX*, *comEC*, *comEA*, *comF*, *comM*, and *dprA*) regulating the formation of natural competence of *V. vulnificus*.[18,35] Gene *tofX* encodes the major activator that controls the development of competence in *V. vulnificus*.[18] Gene *comEA* encodes the periplasmic protein that binds and directs DNA to the inner membrane channels.[18] Genes *comEC*, *comF*, and *comM* encode inner membrane channel genes.[18,35] Gene *dprA* encodes the DNA processing protein that protects incoming DNA from degradation.[36,37] The 16S rRNA gene, which exhibits relatively stable expression in bacteria, was used as the reference gene for gene expression normalization.[38]

Bacterial samples were subjected to RNA extraction, purification, and quantification using the RNAprep pure Cell Kit (Tiangen Biotech, China) following the manufacturer's instructions. Subsequently, a reverse transcription−polymerase chain reaction (RT-PCR) analysis was conducted to obtain the cDNA with a FastKing RT Kit (Tiangen Biotech, China). Triplicate qPCR reactions were conducted to identify the cycle

https://doi.org/10.1021/acs.est.2c06158
Environ. Sci. Technol. 2022, 56, 17166−17176

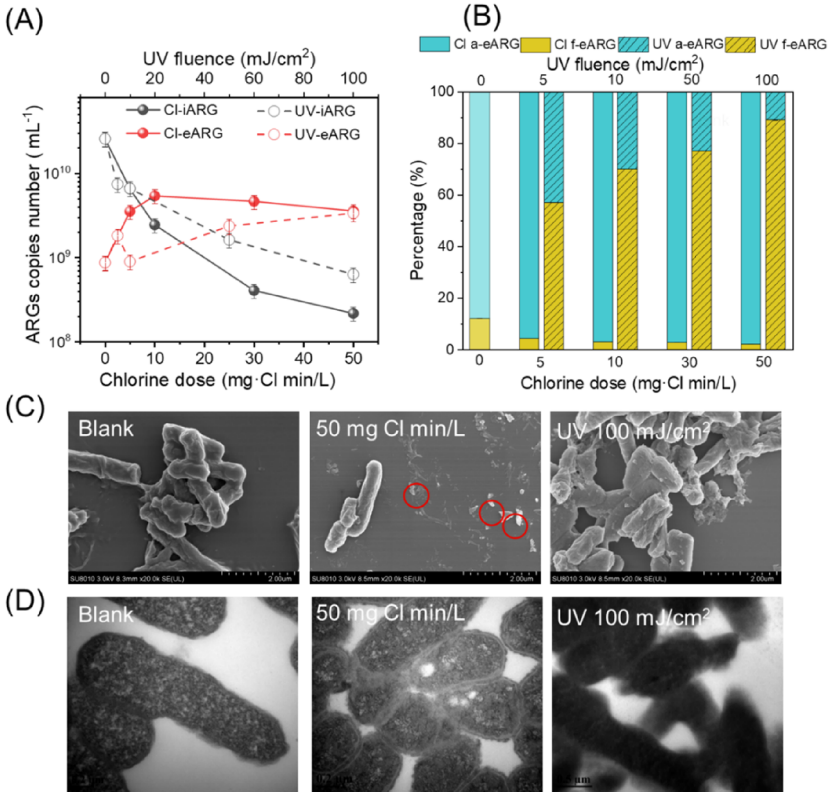

Figure 1. Chlorination induced a significant increase in debris-adsorbed eARG (a-eARG) abundance, while UV irradiation released predominantly free eARGs (f-eARGs). (A) Changes in the relative abundance of iARG and eARG during chlorination and UV irradiation. (B) Changes in the relative proportion of a-eARG and f-eARG during chlorination and UV irradiation. (C) The morphology of bacterial debris after chlorination and UV irradiation as shown by SEM. The red circle highlights the generation of bacterial debris after chlorination especially at high doses. (D) TEM images show aggregation of bacterial debris after chlorination while the bacterial debris became more rigid after UV irradiation. Error bars in all figures represent standard deviations between triplicate tests for each assay (n = 3).

threshold (CT) values for the target and reference genes, and the $2^{-\Delta\Delta CT}$ method was used to quantify the differential gene expression relative to the reference gene.[39] Detailed information about primers is listed in Table S2.

ARG Propagation and Decay Tests in Receiving Water. The wastewater treatment plant secondary effluent was centrifuged and filtered to remove bacteria and associated iARGs. The filtrate containing free eARGs was spiked into the receiving river water (characterized in Table S1) and incubated with different types of bacterial debris for 6 h at room temperature. Bacterial debris of *E. coli* suspensions (~10^8 CFU/mL) were produced by chlorination or UV disinfection as described in the previous section. The added bacterial debris accounted for less than 10% of total suspended solids in the receiving water. Changes in the abundance of common ARGs (i.e., *tetA*, *tetX*, *sulI*, and bla_{NDM-1}) were examined. The persistence of adsorbed and free eARGs in receiving water was also examined under light conditions; details are given in Text S8.

Statistical Analyses. All the experiments were performed independently in at least triplicate. ANOVA and Student's t-test with Bonferonni correction for multiple comparisons were used to determine statistical significance ($p < 0.05$).

RESULTS AND DISCUSSION

Chlorination Predominantly Generates Debris-Adsorbed eARGs, while UV Irradiation Resulted in Free eARGs. Some eDNA can attach on the surface of pristine bacteria despite thoroughly washing before disinfection, so both f-eARG and a-eARG were detected with a-eARG as the dominant form before disinfection. Both chlorination (5−50 mg min/L) and UV irradiation (5−100 mJ/cm^2) were efficient at killing ARB as shown by the 2.9−6.9 log and 3.1−7.5 log reduction, respectively (Figure S2). Thus, iARG levels decreased with longer disinfection time (Figure 1A). Though ARGs were significantly degraded as reflected by a decrease in the total ARG abundance (e.g., by 62−86% after chlorination and 66−85% after UV disinfection), some iARGs were not efficiently degraded but rather released as eARGs whose levels increased with disinfection time (Figure 1A). Chlorination disrupts the cell wall and facilitates cell lysis, while UV irradiation inactivates bacteria mainly by extensive genome damage.[9] Accordingly, the chlorine-treated ARB released eARGs more rapidly relative to UV-treated ARB (first-order rate constant of 0.49 ± 0.03/min for chlorination vs 0.21 ± 0.02/min for UV irradiation). Interestingly, the percentage of adsorbed eARGs increased with the chlorine dosage, while eARGs released after UV irradiation mainly remained as free eARGs (Figure 1B). After chlorination at 50 mg min/L, eARGs were predominantly adsorbed (98% of total eARGs), while UV irradiation at 100 mJ/cm^2 resulted in predominantly free eARGs (89% of total eARGs).

The different physical states of released eARGs are likely due to the different bacterial debris properties after these two disinfection processes (Figure 1C,D and Figures S3 and S4). Specifically, bacterial cells were damaged after chlorination, generating debris with sizes ranging from 99 to 27 nm at 50 mg

https://doi.org/10.1021/acs.est.2c06158
Environ. Sci. Technol. 2022, 56, 17166−17176

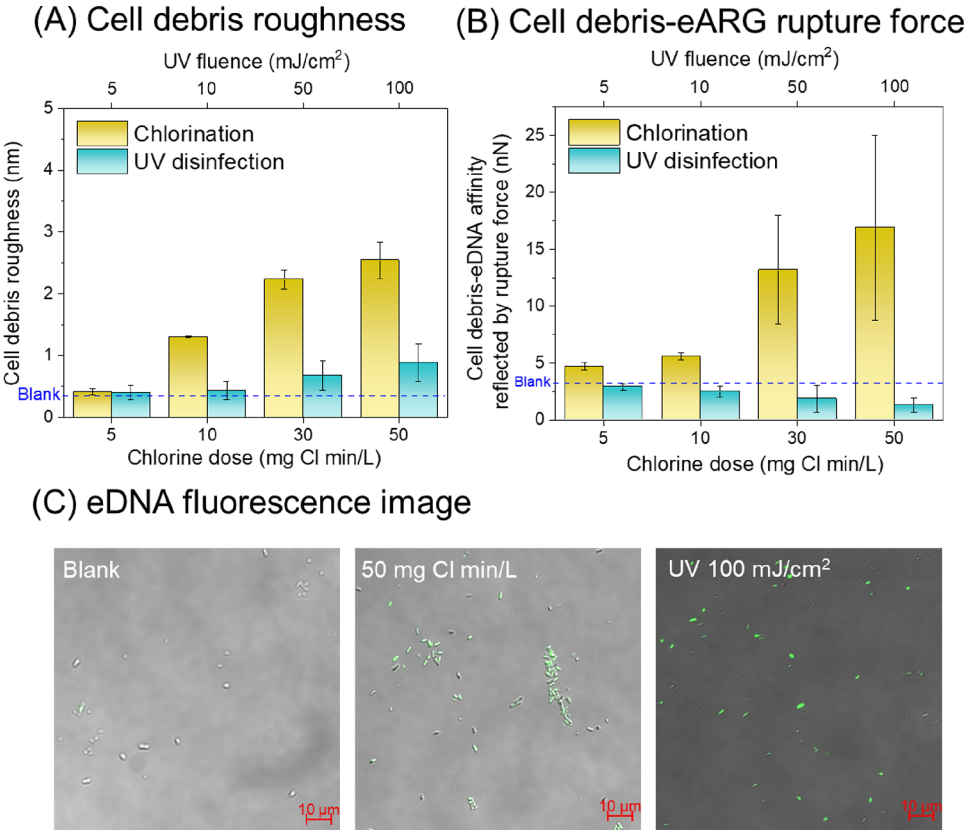

Figure 2. Chlorination and UV generate bacterial debris with distinct properties that interact with eARGs differently. (A) Changes in the roughness of bacterial debris after chlorination and UV irradiation. (B) Changes in the rupture force between eARGs and cell debris after chlorination or UV irradiation. (C) eDNA fluorescence imaging in samples before and after chlorination and UV irradiation.

min/L (Figure S5). In contrast, most bacteria remained intact post UV irradiation (Figure 1C,D and Figures S3 and S4) with slight changes in the bacterial size distribution (Figure S5). Moreover, the bacterial debris surface became 6.7 times rougher after chlorination at 50 mg min/L compared to undisinfected bacteria, according to AFM measurements (Figure 2A). In contrast, the roughness of bacterial debris only increased by 2.3-fold after UV irradiation at 100 mJ/cm^2. Accordingly, AFM force−distance curves revealed increased bacteria affinity toward DNA after chlorination but decreased affinity after UV irradiation. Specifically, the bacterial surface-DNA rupture force increased from 2.9 ± 0.3 to 16.9 ± 8.1 nN after chlorination (50 mg min/L) but decreased after UV irradiation (100 mJ/cm^2) to 1.3 ± 0.7 nN (Figure 2B). The rougher surface and higher affinity for eDNA (Figure 2A,B) contributed to the accumulation of eDNA onto bacterial debris after chlorination, as visualized by florescence microscopy (Figure 2C). In contrast, much less eDNA was adsorbed by debris after UV disinfection (Figure 2C), possibly due to a lower roughness and eDNA affinity (Figure 2A,B).

Chlorination can oxidize cell-wall materials such as N-terminal amino groups of proteins and induce side-chain modification, backbone fragmentation, and cross-linking,[40] resulting in a rough and wrinkled surface that facilitates DNA attachment. The FTIR spectrum demonstrated an increased extent of cell surface oxidation after both chlorination and UV irradiation. However, more oxidized groups were generated by chlorination as reflected by the higher intensity of −COOH (Figure S6), which was corroborated by a higher O/C ratio observed by XPS (Table S3). Additional chlorinated functional groups (potentially −NHCl or $-NCl_2$[41]) could result in less negatively charged bacterial debris (Table S3), while UV irradiation resulted in a more negatively charged bacterial surface (Table S3). Furthermore, the bacterial debris became more rigid post UV irradiation (Figure 1D) with significant decreases in fluidity (2.3-fold by 100 mJ/cm^2) compared to the blank control (Figure 5B), potentially due to the lipid peroxidation.[42]

Debris-Associated eARGs Exhibited a Higher Transformation Frequency than That of Free eARGs. Whereas conjugation and transduction are recognized as the dominant mechanisms of horizontal gene transfer (HGT) in various environments, transformation is also an important HGT mechanism that should not be overlooked when both eARGs and competent bacteria co-exist in high concentrations.[10] Chlorination and UV irradiation resulted in a significant difference in eARG transformation efficiency (Figure 3). The transformation frequency of f-eARGs was significantly enhanced after adsorbing to intact bacteria (by 1.6-fold for natural transformation and 2.7-fold for chemical transformation) (Figure 3A,C). This phenomenon was also reported for other substances such as microplastics[10] and solid particles in water by attaching eARGs. Furthermore, bacterial debris produced by chlorination enhanced both chemical and natural transformation of eARGs. Specifically, at doses higher than 30 mg min/L when bacterial debris are prevalent, the transformation frequency for the same eARG concentration increased significantly relative to the free eARGs by 7.2-fold for natural transformation and 11.3-fold for chemical transformation at 50 mg min/L (Figure 3A,C). In

https://doi.org/10.1021/acs.est.2c06158
Environ. Sci. Technol. 2022, 56, 17166−17176

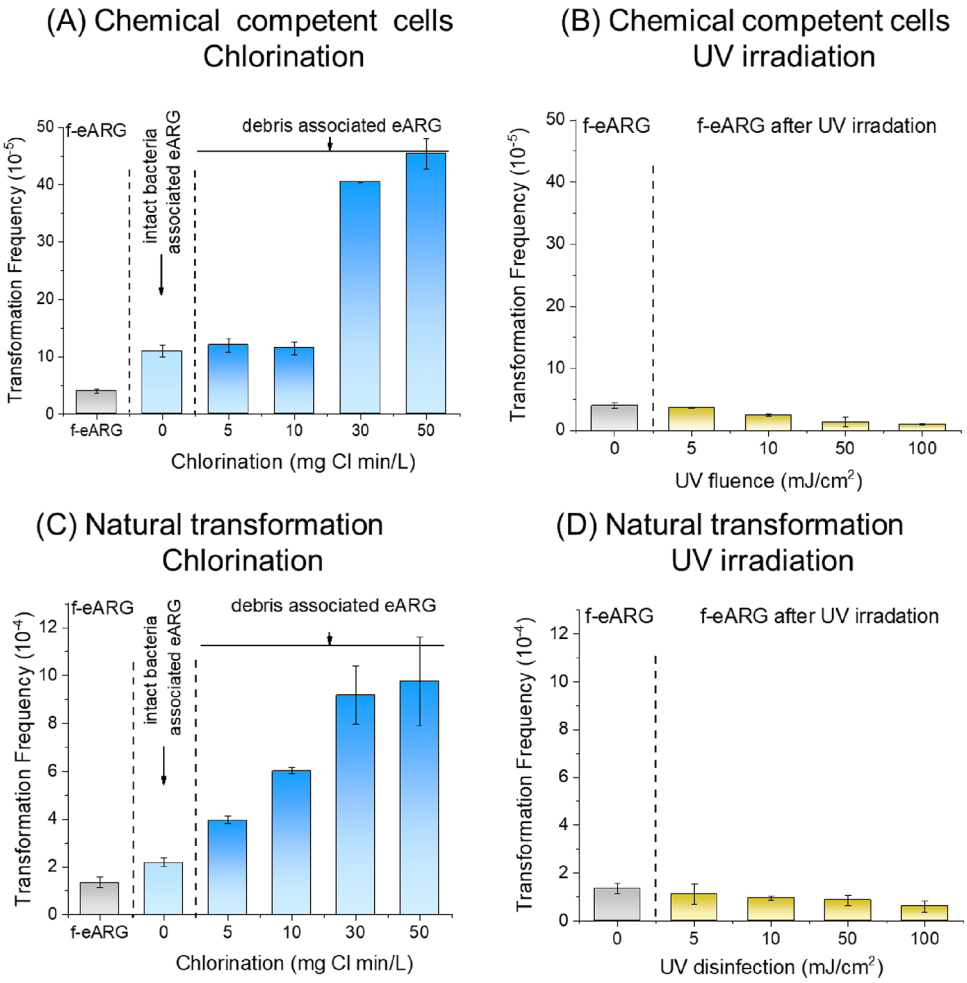

Figure 3. Chlorination-produced adsorbed eARGs exhibited a higher transformation frequency than that of free eARGs. (A) Transformation frequency of f-eARG and a-eARG associated with bacterial debris produced by chlorination at various doses by reference strain *E. coli* HB101. (B) Transformation frequency of f-eARG after exposure to UV irradiation at various fluences by reference strain *E. coli* HB101. (C) Transformation frequency of f-eARG and a-eARG associated with bacterial debris produced by chlorination at various doses by natural competent strain *V. vulnificus*. (D) Transformation frequency of f-eARG after exposure to UV irradiation at various fluences by natural competent strain *V. vulnificus*.

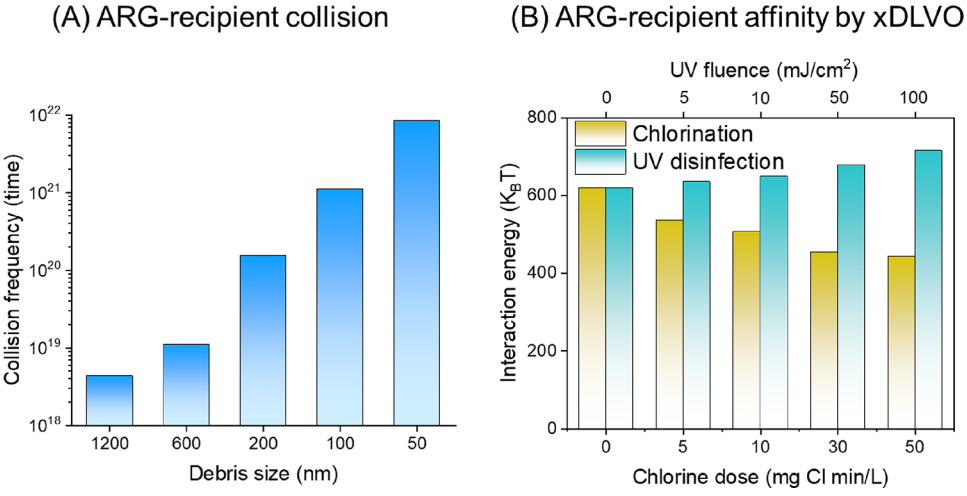

Figure 4. Simulation of ARG donor−recipient interactions. (A) Collision frequency between eARGs adsorbed to chlorination-generated bacterial debris and recipient cells during transformation events. (B) Interaction energy between the a-eARG and recipient before and after chlorination and UV irradiation based on xDLVO theory.

contrast, both the natural and chemical transformation frequency of UV irradiation-derived eARGs decreased as the disinfection intensity increased from 0 to 100 mJ/cm^2 (Figure 3B,D), suggesting that, in addition to ARB inactivation, UV

https://doi.org/10.1021/acs.est.2c06158
Environ. Sci. Technol. 2022, 56, 17166−17176

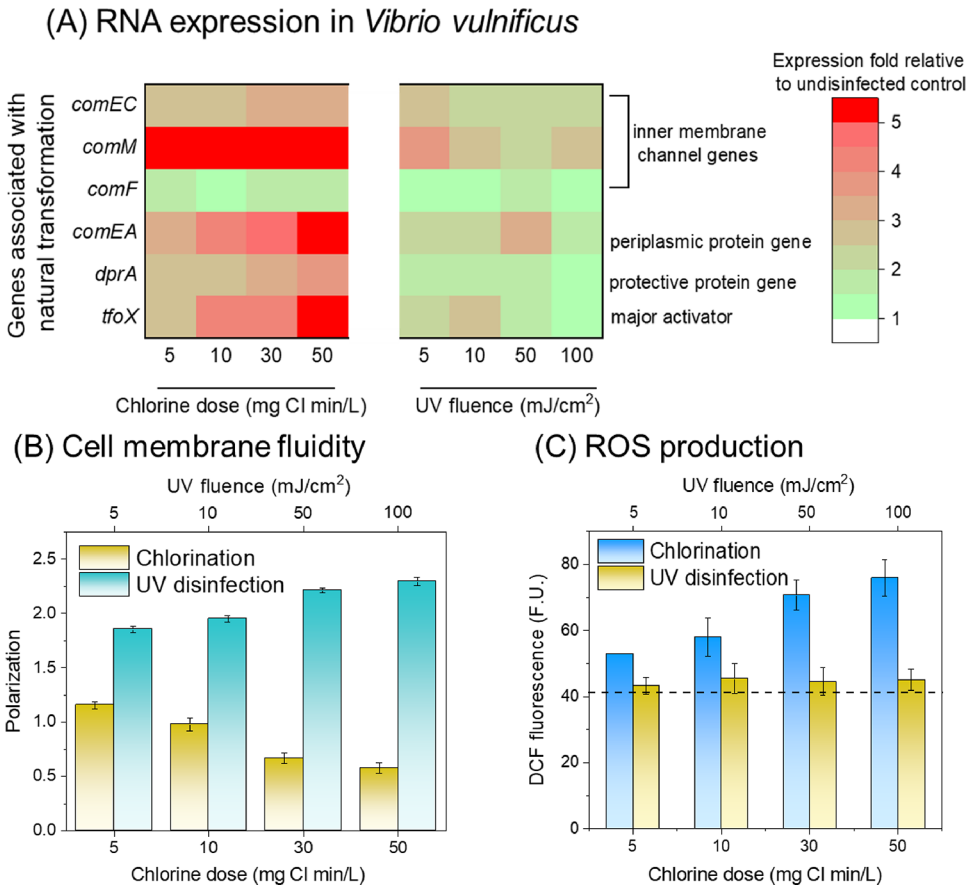

Figure 5. Recipient bacteria upregulated transformation genes after exposure to chlorination-generated bacterial debris. (A) Expression of *V. vulnificus* genes associated with natural transformation after exposure to bacterial debris generated by chlorination or UV irradiation at various intensities. (B) Changes in the cell membrane fluidity after treatment by chlorination or UV irradiation at various intensities. (C). Intracellular ROS production by *V. vulnificus* exposed to bacterial debris generated after chlorination or UV disinfection at various intensities. The dashed line represents baseline ROS levels in *V. vulnificus* exposed to intact *E. coli* HB101 from which bacterial debris was generated.

irradiation could also mitigate antibiotic resistance dissemination via transformation.

There have been studies showing that chlorination enhanced eARG transformation; the dominant mechanism was the higher susceptibility of recipient bacteria due to increased permeability by residual chlorine.[43,44] Our results show that chlorinated bacterial debris generated by chlorine disinfection could also promote eARG transformation in addition to increasing the permeability of recipient cells. In contrast, the transformation potential by free eARGs, the major type of eARG after UV irradiation (Figure 1B), decreased significantly at all irradiation fluences (by 55% at 100 mJ/cm^2 relative to undisinfected control) and chemical transformation (by 81% at 100 mJ/cm^2). This is apparently due to the damage on eARGs that lost the ability to express antibiotic resistance.

Increased Donor−Recipient Collision and Upregulation of Transformation Genes Contributed to Enhanced Natural Transformation by Debris-Adsorbed eARGs. Transformation of eARGs by recipient bacteria occurs in three steps: eARG−recipient contact, eARG uptake, and eARG expression. Bacterial debris exhibited high affinity to both eARGs and recipient bacteria and thus could facilitate eARG−recipient contact. In fact, the presence of 200 nm bacterial debris significantly enhanced eARG−recipient contact frequency by 35.1-fold relative to the original (undisinfected) intact bacteria (1200 nm) (Figure 4A). Additionally, the xDLVO model suggests that bacterial debris generated by chlorination (50 mg min/L) decreased the energy barrier between the donor (eARG) and recipient (bacteria) by 29% (Figure 4B). In contrast, bacterial debris after UV irradiation increased the energy barrier by 15% (at 100 mJ/cm^2) due to the decreased cell membrane fluidity and increased electrostatic repulsion (as indicated by zeta potential) of bacterial debris (Table S3), which significantly decreased the transformation frequency (by 55% at 100 mJ/cm^2 for natural transformation and 81% for chemical transformation relative to undisinfected control).

Transcriptomic analysis showed that genes related to natural transformation in *V. vulnificus* were significantly upregulated by bacterial debris generated by chlorination. The major activator *tofX* of natural transformation in *V. vulnificus* was elevated by 2.6−5.2-fold relative to the undisinfected control (Figure 5A). This upregulation also extended to other related genes including the periplasmic protein gene (*comEA*, 3.4 to 6.4-fold increase), inner membrane channel genes (*comEC*, 2.7−3.4-fold increase; *comF*, 1.5−1.8-fold increase; and *comM* 5.3−6.9-fold increase), and the protective protein gene (*dprA*, 2.9−3.9-fold increase). In contrast, UV irradiation resulted in a much lesser upregulation (1.4 to 2.5-fold for *tofX*) than chlorination.

This upregulation by chlorination-generated bacterial debris (Figure 5A) is likely partially caused by free radicals, which are

https://doi.org/10.1021/acs.est.2c06158
Environ. Sci. Technol. 2022, 56, 17166−17176

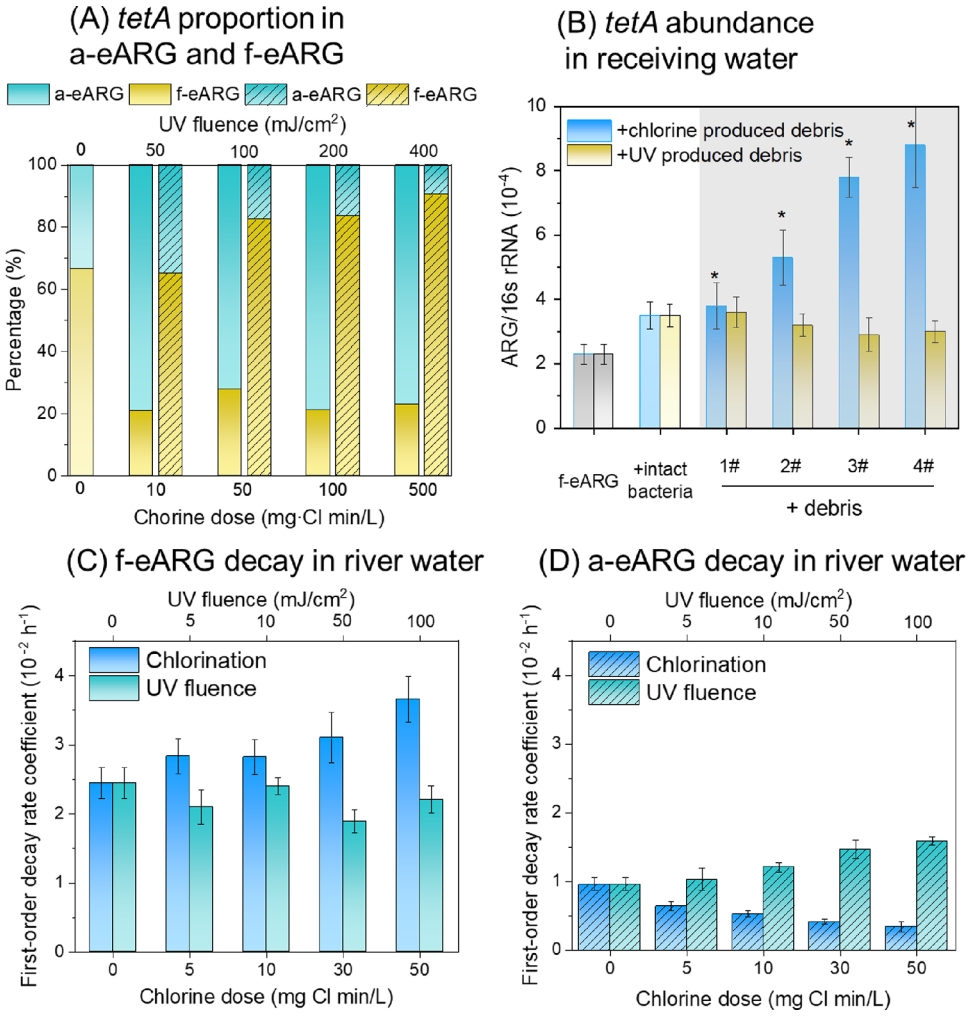

Figure 6. (A) Changes in the relative proportion of adsorbed and free extracellular *tetA* during chlorination and UV irradiation of the secondary effluent. (B). Changes in the relative abundance of *tetA* (i.e., *tetA*/16 s rRNA) in receiving water when eDNA from the secondary effluent was spiked and incubated for 6 h. Intact untreated bacteria and bacterial debris generated by chlorination and UV irradiation were spiked in receiving water during the experiment. Numbers 1−4 represent bacterial debris generated by chlorination at various doses (5, 10, 30, or 50 mg min/L) or UV irradiation at various fluences (5, 10, 50, or 100 mJ/cm^2). First-order decay rate coefficient of the f-eARG (C) and a-eARG (D) after chlorination and UV irradiation in river water in the presence of simulated sunlight.

known to contribute to enhanced HGT through upregulation of transformation-associated genes.[45] Notably, the amount of persistent free radicals became more abundant in bacterial debris post chlorination than post UV irradiation (e.g., 8.1 × 10^{12} spins/g at 50 mg min/L vs 4.7 × 10^{12} spins/g at 100 mJ/cm^2) (Figure S7). Another factor contributing to upregulation of genes associated with natural transformation is likely the generation of chlorinated organic molecules.[3,46] IC analysis showed that a 5.1-fold higher Cl content was observed after chlorination at 50 mg min/L compared to the undisinfected control (Table S3). Furthermore, the increased cell membrane fluidity (e.g., by 1.7-fold at 50 mg min/L compared to undisinfected control) enhanced the impact of bacterial debris containing persistent free radicals toward recipients (Figure 5B). In contrast, the fluidity of bacterial debris significantly decreased after UV irradiation (e.g., by 57% at 100 mJ/cm^2) (Figure 5B), which confined the impact of free radicals toward recipients. A significantly higher ROS abundance was also observed for *V. vulnificus* after exposure to bacterial debris produced by chlorination (up to 1.8-fold) rather than UV disinfection (Figure 5C). Bacterial debris after chlorination has also been reported to contain chlorinated groups such as chloramines,[37] which could upregulate the expression of HGT-related genes[43] and thus be conductive to enhanced transformation.

Adsorbed eARGs Had a Higher Propagation Rate and Persistence Compared to Free eARGs. The prevalence of physical states of representative eARGs, including *tetA*, *tetX*, *sulI*, and bla_{NDM-1}, in the secondary effluent was examined. Chlorination (500 mg min/L) again predominantly generated adsorbed eARGs (77−98% of total eARGs), while UV irradiation (400 mJ/cm^2) predominantly released free eARGs (81%−94% of total eARGs) (Figure 6A and Figure S8). The release of eDNA from the secondary effluent contributed to the slight 1.1−1.5-fold increase of ARG abundance in the receiving water. This is likely caused by transformation and replication of eARGs in the receiving water bacteria. Furthermore, chlorination-generated bacterial debris significantly enhanced ARG propagation in the receiving water by 2.0−4.6-fold for *tetA*, 1.4−4.9-fold for *tetX*, 1.3−2.8-fold for *sulI*, and 1.8−7.8-fold for bla_{NDM-1} (Figure 6B and Figure S9).

https://doi.org/10.1021/acs.est.2c06158
Environ. Sci. Technol. 2022, 56, 17166−17176

Despite having a much smaller surface area than that of the more abundant background suspended solids (8.6 ± 0.3 mg/L in receiving water, Table S1), the bacterial debris was the major determinant for the above results since background suspended solids were present in all groups. Apparently, this disproportionate importance of bacterial debris (less than 10% of total suspended solids; Table S1) is due to (as yet undetermined) surface properties imparted by chlorination. In contrast, bacterial debris post UV irradiation did not significantly enhance the propagation of ARG (i.e., *tetA*) compared to the undisinfected control (Figure 6B).

The presence of bacterial debris produced by chlorination also enhanced the persistence of adsorbed eARG in receiving waters (Figure 6C,D). Natural attenuation of eARGs in river water caused by hydrolysis and photolysis generally followed first-order kinetics. The decay rate coefficient of free eARGs after UV (100 mJ/cm^2) was slightly lower than the untreated controls ($2.2 \pm 0.2 \times 10^{-3}$ h^{-1} vs $2.5 \pm 0.2 \times 10^{-3}$ h^{-1}) (Figure 6C). However, the first-order decay rate coefficient of free eARGs after chlorination increased with the disinfection intensity to $3.7 \pm 0.3 \times 10^{-3}$ h^{-1} at 50 mg min/L, while that for adsorbed eARGs decreased to $0.3 \pm 0.08 \times 10^{-3}$ h^{-1} (Figure 6D). The higher persistence of adsorbed eARGs after chlorination is consistent with the higher affinity of bacterial debris toward eARGs.

Environmental Implications. Wastewater disinfection is an important practice to mitigate the spread of waterborne infectious diseases and control the potential release of antibiotic-resistant pathogens. However, an overlooked unintended consequence of chlorination, which is the dominant effluent disinfection process,[47] is the release eARGs that are predominantly adsorbed to the generated cell debris. This debris has high affinity to both eARGs and recipient bacteria, enhancing opportunities for their effective collision and resulting transformation. Chlorination also produces persistent free radicals and chlorinated molecules on the cell debris that contribute to upregulation of transformation-related genes and further facilitate the horizontal transfer of the adsorbed eARGs. This combination of the active surface area for proximal adsorption of transforming eDNA and recipient cells and generating transformation-enhancing substrates could lead to an enrichment of the environmental resistome even in the absence of antibiotics. In contrast, disinfection by UV irradiation releases mainly free (possibly damaged) eARGs with a significantly lower transformation potential.

Overall, eARGs adsorbed to bacterial debris generated by chlorination is likely to experience higher persistence and a higher propagation potential than free eARGs in receiving waters. However, further studies at larger temporal and spatial scales are needed to determine whether this effect contributes significantly to resistome dissemination.

■ ASSOCIATED CONTENT

Supporting Information

The Supporting Information is available free of charge at https://pubs.acs.org/doi/10.1021/acs.est.2c06158.

Descriptions of methods of eDNA extraction, qPCR, zeta potential, and contact angle measurements, functionalization of AFM, force−distance measurements, xDLVO, and chemical transformation. Verification of transformants, inactivation of *E. coli* HB101 by disinfection, SEM and TEM images of bacterial debris, and detection of bacterial debris sizes, FTIR, and free radicals (PDF)

■ AUTHOR INFORMATION

Corresponding Authors

Pingfeng Yu − *College of Environment and Resource Sciences, Zhejiang University, Hangzhou 310058, China;* orcid.org/0000-0003-0402-773X; Email: yupf@zju.edu.cn

Pedro J. J. Alvarez − *Department of Civil and Environmental Engineering, Rice University, Houston 77005 Texas, United States;* orcid.org/0000-0002-6725-7199; Email: alvarez@rice.edu

Authors

Qingbin Yuan − *State Key Laboratory of Pollution Control and Resource Reuse, School of the Environment, Nanjing University, Nanjing 210023, China; School of Environmental Science and Engineering, Nanjing Tech University, Nanjing 211816, China*

Yuan Cheng − *School of Environmental Science and Engineering, Nanjing Tech University, Nanjing 211816, China*

Pengxiao Zuo − *Department of Civil and Environmental Engineering, Rice University, Houston 77005 Texas, United States*

Yisi Xu − *School of Environmental Science and Engineering, Nanjing Tech University, Nanjing 211816, China*

Yuxiao Cui − *College of Environmental Science and Engineering, Nankai University, Tianjin 300071, China*

Yi Luo − *State Key Laboratory of Pollution Control and Resource Reuse, School of the Environment, Nanjing University, Nanjing 210023, China*

Complete contact information is available at: https://pubs.acs.org/10.1021/acs.est.2c06158

Notes

The authors declare no competing financial interest.

■ ACKNOWLEDGMENTS

This work was supported by the National Natural Science Foundation of China (grant no. 42177348), Natural Science Foundation of Jiangsu Province (grant no. BK20201367), China Postdoctoral Science Foundation (grant no. 2021 M701663), Key Program of the National Natural Science Foundation of China (grant no. 52030003), and NSF ERC on Nanotechnology-Enabled Water Treatment (no. EEC-1449500), We thank Ruonan Sun and Dan Huang for their help on experimental design and data analysis.

■ REFERENCES

(1) Murray, C. J. L.; Ikuta, K. S.; Sharara, F.; Swetschinski, L.; Robles Aguilar, G.; Gray, A.; Han, C.; Bisignano, C.; Rao, P.; Wool, E.; Johnson, S. C.; Browne, A. J.; Chipeta, M. G.; Fell, F.; Hackett, S.; Haines-Woodhouse, G.; Kashef Hamadani, B. H.; Kumaran, E. A. P.; McManigal, B.; Agarwal, R.; Akech, S.; Albertson, S.; Amuasi, J.; Andrews, J.; Aravkin, A.; Ashley, E.; Bailey, F.; Baker, S.; Basnyat, B.; Bekker, A.; Bender, R.; Bethou, A.; Bielicki, J.; Boonkasidecha, S.; Bukosia, J.; Carvalheiro, C.; Castañeda-Orjuela, C.; Chansamouth, V.; Chaurasia, S.; Chiurchiù, S.; Chowdhury, F.; Cook, A. J.; Cooper, B.; Cressey, T. R.; Criollo-Mora, E.; Cunningham, M.; Darboe, S.; Day, N. P. J.; De Luca, M.; Dokova, K.; Dramowski, A.; Dunachie, S. J.; Eckmanns, T.; Eibach, D.; Emami, A.; Feasey, N.; Fisher-Pearson, N.;

Forrest, K.; Garrett, D.; Gastmeier, P.; Giref, A. Z.; Greer, R. C.; Gupta, V.; Haller, S.; Haselbeck, A.; Hay, S. I.; Holm, M.; Hopkins, S.; Iregbu, K. C.; Jacobs, J.; Jarovsky, D.; Javanmardi, F.; Khorana, M.; Kissoon, N.; Kobeissi, E.; Kostyanev, T.; Krapp, F.; Krumkamp, R.; Kumar, A.; Kyu, H. H.; Lim, C.; Limmathurotsakul, D.; Loftus, M. J.; Lunn, M.; Ma, J.; Mturi, N.; Munera-Huertas, T.; Musicha, P.; Mussi-Pinhata, M. M.; Nakamura, T.; Nanavati, R.; Nangia, S.; Newton, P.; Ngoun, C.; Novotney, A.; Nwakanma, D.; Obiero, C. W.; Olivas-Martinez, A.; Olliaro, P.; Ooko, E.; Ortiz-Brizuela, E.; Peleg, A. Y.; Perrone, C.; Plakkal, N.; Ponce-de-Leon, A.; Raad, M.; Ramdin, T.; Riddell, A.; Roberts, T.; Robotham, J. V.; Roca, A.; Rudd, K. E.; Russell, N.; Schnall, J.; Scott, J. A. G.; Shivamallappa, M.; Sifuentes-Osornio, J.; Steenkeste, N.; Stewardson, A. J.; Stoeva, T.; Tasak, N.; Thaiprakong, A.; Thwaites, G.; Turner, C.; Turner, P.; van Doorn, H. R.; Velaphi, S.; Vongpradith, A.; Vu, H.; Walsh, T.; Waner, S.; Wangrangsimakul, T.; Wozniak, T.; Zheng, P.; Sartorius, B.; Lopez, A. D.; Stergachis, A.; Moore, C.; Dolecek, C.; Naghavi, M. Global burden of bacterial antimicrobial resistance in 2019: a systematic analysis. *Lancet* **2022**, *399*, 629−655.

(2) Wei, Z.; Feng, K.; Wang, Z.; Zhang, Y.; Yang, M.; Zhu, Y.-G.; Virta, M. P. J.; Deng, Y. High-throughput single-cell technology reveals the contribution of horizontal gene transfer to typical antibiotic resistance gene dissemination in wastewater treatment plants. *Environ. Sci. Technol.* **2021**, *55*, 11824−11834.

(3) Zammit, I.; Marano, R. B. M.; Vaiano, V.; Cytryn, E.; Rizzo, L. Changes in antibiotic resistance gene levels in soil after irrigation with treated wastewater: A comparison between heterogeneous photocatalysis and Chlorination. *Environ. Sci. Technol.* **2020**, *54*, 7677−7686.

(4) Yuan, Q.-B.; Huang, Y.-M.; Wu, W.-B.; Zuo, P.; Hu, N.; Zhou, Y.-Z.; Alvarez, P. J. J. Redistribution of intracellular and extracellular free & adsorbed antibiotic resistance genes through a wastewater treatment plant by an enhanced extracellular DNA extraction method with magnetic beads. *Environ. Int.* **2019**, *131*, No. 104986.

(5) Liu, S. S.; Qu, H. M.; Yang, D.; Hu, H.; Liu, W. L.; Qiu, Z. G.; Hou, A. M.; Guo, J.; Li, J. W.; Shen, Z. Q.; Jin, M. Chlorine disinfection increases both intracellular and extracellular antibiotic resistance genes in a full-scale wastewater treatment plant. *Water Res.* **2018**, *136*, 131−136.

(6) Mao, D.; Luo, Y.; Mathieu, J.; Wang, Q.; Feng, L.; Mu, Q.; Feng, C.; Alvarez, P. J. J. Persistence of extracellular DNA in river sediment facilitates antibiotic resistance gene propagation. *Environ. Sci. Technol.* **2014**, *48*, 71−78.

(7) Calderón-Franco, D.; van Loosdrecht, M. C. M.; Abeel, T.; Weissbrodt, D. G. Free-floating extracellular DNA: Systematic profiling of mobile genetic elements and antibiotic resistance from wastewater. *Water Res.* **2021**, *189*, No. 116592.

(8) Zhang, Y. Y.; Zhuang, Y.; Geng, J. J.; Ren, H. Q.; Zhang, Y.; Ding, L. L.; Xu, K. Inactivation of antibiotic resistance genes in municipal wastewater effluent by chlorination and sequential UV/chlorination disinfection. *Sci. Total Environ.* **2015**, *512*, 125−132.

(9) He, H.; Zhou, P.; Shimabuku, K. K.; Fang, X.; Li, S.; Lee, Y.; Dodd, M. C. Degradation and deactivation of bacterial antibiotic resistance genes during exposure to free chlorine, monochloramine, chlorine dioxide, ozone, ultraviolet light, and hydroxyl radical. *Environ. Sci. Technol.* **2019**, *53*, 2013−2026.

(10) Yuan, Q.; Sun, R.; Yu, P.; Cheng, Y.; Wu, W.; Bao, J.; Alvarez, P. J. J. UV-aging of microplastics increases proximal ARG donor-recipient adsorption and leaching of chemicals that synergistically enhance antibiotic resistance propagation. *J. Hazard. Mater.* **2022**, No. 127895.

(11) Venkobachar, C.; Iyengar, L.; Prabhakara Rao, A. V. S. Mechanism of disinfection: Effect of chlorine on cell membrane functions. *Water Res.* **1977**, *11*, 727−729.

(12) Coombs, M. M.; Danielli, J. F. Chlorination of Proteins as a Method of increasing their Opacity in the Electron Microscope. *Nature* **1959**, *183*, 1257−1258.

(13) Gibson, J.; Drake, J.; Karney, B.UV disinfection of wastewater and combined sewer overflows. In *Ultraviolet Light in Human Health, Diseases and Environment*;Springer, Cham: 2017, 267−275.

(14) Yang, L.; Liu, G.; Zheng, M.; Jin, R.; Zhao, Y.; Wu, X.; Xu, Y. Pivotal roles of metal oxides in the formation of environmentally persistent free radicals. *Environ. Sci. Technol.* **2017**, *51*, 12329−12336.

(15) Shang, C.; Blatchley, E. R. Chlorination of pure bacterial cultures in aqueous solution. *Water Res.* **2001**, *35*, 244−254.

(16) Du, Y.; Wang, W.-L.; He, T.; Sun, Y.-X.; Lv, X.-T.; Wu, Q.-Y.; Hu, H.-Y. Chlorinated effluent organic matter causes higher toxicity than chlorinated natural organic matter by inducing more intracellular reactive oxygen species. *Sci. Total Environ.* **2020**, *701*, No. 134881.

(17) Gulig, P. A.; Tucker, M. S.; Thiaville, P. C.; Joseph, J. L.; Brown, R. N. USER friendly cloning coupled with chitin-based natural transformation enables rapid mutagenesis of Vibrio vulnificus. *Appl. Environ. Microbiol.* **2009**, *75*, 4936−4949.

(18) Simpson, C. A.; Podicheti, R.; Rusch, D. B.; Dalia, A. B.; van Kessel, J. C. Diversity in natural transformation frequencies and regulation across *Vibrio* Species. *MBio* **2019**, *10*, e02788-19.

(19) Abioye, O. E.; Osunla, A. C.; Okoh, A. I. Molecular detection and distribution of six medically important *Vibrio* spp. In selected freshwater and brackish water resources in Eastern Cape Province, South Africa. *Front. Microbiol.* **2021**, *12*, No. 617703.

(20) Mantilla-Calderon, D.; Plewa, M. J.; Michoud, G.; Fodelianakis, S.; Daffonchio, D.; Hong, P.-Y. Water Disinfection Byproducts Increase Natural Transformation Rates of Environmental DNA in Acinetobacter baylyi ADP1. *Environ. Sci. Technol.* **2019**, *53*, 6520−6528.

(21) Yuan, Q.; Zhang, D.; Yu, P.; Sun, R.; Javed, H.; Wu, G.; Alvarez, P. J. J. Selective adsorption and photocatalytic degradation of extracellular antibiotic resistance genes by molecularly-imprinted graphitic carbon nitride. *Environ. Sci. Technol.* **2020**, *54*, 4621−4630.

(22) Guo, M. T.; Yuan, Q. B.; Yang, J. Distinguishing Effects of Ultraviolet Exposure and Chlorination on the Horizontal Transfer of Antibiotic Resistance Genes in Municipal Wastewater. *Environ. Sci. Technol.* **2015**, *49*, 5771−5778.

(23) He, H.; Zhou, P.; Shimabuku, K. K.; Fang, X.; Li, S.; Lee, Y.; Dodd, M. C. Degradation and Deactivation of Bacterial Antibiotic Resistance Genes during Exposure to Free Chlorine, Monochloramine, Chlorine Dioxide, Ozone, Ultraviolet Light, and Hydroxyl Radical. *Environ. Sci. Technol.* **2020**, *54*, 10975−10975.

(24) Sun, H.; Li, G.; Nie, X.; Shi, H.; Wong, P.-K.; Zhao, H.; An, T. Systematic approach to in-depth understanding of photoelectrocatalytic bacterial inactivation mechanisms by tracking the decomposed building blocks. *Environ. Sci. Technol.* **2014**, *48*, 9412−9419.

(25) Liu, S.; Shen, Z.; Wu, B.; Yu, Y.; Hou, H.; Zhang, X.-X.; Ren, H.-q. Cytotoxicity and efflux pump inhibition induced by molybdenum disulfide and boron nitride nanomaterials with sheetlike structure. *Environ. Sci. Technol.* **2017**, *51*, 10834−10842.

(26) Echigo, S.; Zhang, X.; Minear, R. A.; Plewa, M. J., Differentiation of Total Organic Brominated and Chlorinated Compounds in Total Organic Halide Measurement: A New Approach with an Ion-Chromatographic Technique. In *Natural Organic Matter and Disinfection By-Products*; American Chemical Society: 2000; Vol. *761*, pp. 330−342.

(27) Liu, Z.; Sun, Y.; Wang, J.; Li, J.; Jia, H. In Vitro assessment reveals the effects of environmentally persistent free radicals on the toxicity of photoaged tire wear particles. *Environ. Sci. Technol.* **2022**, *56*, 1664−1674.

(28) Basnar, B.; Elnathan, R.; Willner, I. Following aptamer−thrombin binding by force measurements. *Anal. Chem.* **2006**, *78*, 3638−3642.

(29) Liu, J.; Zhang, T.; Tian, L.; Liu, X.; Qi, Z.; Ma, Y.; Ji, R.; Chen, W. Aging significantly affects mobility and contaminant-mobilizing ability of nanoplastics in saturated loamy sand. *Environ. Sci. Technol.* **2019**, *53*, 5805−5815.

(30) Phan, H. T.; Heiderscheit, T. S.; Haes, A. J. Understanding time-dependent surface-enhanced raman scattering from gold nano-

https://doi.org/10.1021/acs.est.2c06158
Environ. Sci. Technol. 2022, 56, 17166−17176

sphere aggregates using collision theory. *J. Phys. Chem. C* **2020**, *124*, 14287−14296.
(31) Sun, R.; Yu, P.; Zuo, P.; Alvarez, P. J. J. Bacterial Concentrations and Water Turbulence Influence the Importance of Conjugation Versus Phage-Mediated Antibiotic Resistance Gene Transfer in Suspended Growth Systems. *ACS Environ. Au* **2022**, *2*, 156−165.
(32) Sikora, A. E., *Vibrio Cholerae*; Humana Press: New York, 2018.
(33) Dalia, T. N.; Hayes, C. A.; Stolyar, S.; Marx, C. J.; McKinlay, J. B.; Dalia, A. B. Multiplex Genome Editing by Natural Transformation (MuGENT) for Synthetic Biology in Vibrio natriegens. *ACS Synth. Biol.* **2017**, *6*, 1650−1655.
(34) Liu, F.; Saavedra, M. G.; Champion, J. A.; Griendling, K. K.; Ng, N. L. Prominent contribution of hydrogen peroxide to intracellular reactive oxygen species generated upon exposure to naphthalene secondary organic aerosols. *Environ. Sci. Technol. Lett.* **2020**, *7*, 171−177.
(35) Lo Scrudato, M.; Blokesch, M. The regulatory network of natural competence and transformation of Vibrio cholerae. *PLoS Genet.* **2012**, *8*, No. e1002778.
(36) Marvig, R. L.; Blokesch, M. Natural transformation of *Vibrio cholerae* as a tool - Optimizing the procedure. *BMC Microbiol.* **2010**, *10*, 155.
(37) Metzger, L. C.; Blokesch, M. Composition of the DNA-uptake complex of *Vibrio cholerae*. *Mobile Genet. Elem.* **2014**, *4*, No. e28142.
(38) Callahan, B. J.; Wong, J.; Heiner, C.; Oh, S.; Theriot, C. M.; Gulati, A. S.; McGill, S. K.; Dougherty, M. K. High-throughput amplicon sequencing of the full-length 16S rRNA gene with single-nucleotide resolution. *Nucleic Acids Res.* **2019**, *47*, No. e103.
(39) Hu, X.; Waigi, M. G.; Yang, B.; Gao, Y. Impact of plastic particles on the horizontal transfer of antibiotic resistance genes to bacterium: Dependent on particle sizes and antibiotic resistance gene vector replication capacities. *Environ. Sci. Technol.* **2022**, DOI: 10.1021/acs.est.2c00745.
(40) Pattison, D. I.; Davies, M. J. Absolute rate constants for the reaction of hypochlorous acid with protein side chains and peptide bonds. *Chem. Res. Toxicol.* **2001**, *14*, 1453−1464.
(41) Egawa, T.; Ito, M.; Konaka, S. Reactions of N, N-dichloroalkylamines with solid base as studied by FTIR combined with DFT calculations. *J. Mol. Struct.* **2001**, *560*, 337−344.
(42) Bose, B.; Agarwal, S.; Chatterjee, S. N. UV-A induced lipid peroxidation in liposomal membrane. *Radiat. Environ. Biophys.* **1989**, *28*, 59−65.
(43) Zhang, S.; Wang, Y.; Lu, J.; Yu, Z.; Song, H.; Bond, P. L.; Guo, J. Chlorine disinfection facilitates natural transformation through ROS-mediated oxidative stress. *ISME J.* **2021**, 2969.
(44) Jin, M.; Liu, L.; Wang, D.-n.; Yang, D.; Liu, W.-l.; Yin, J.; Yang, Z.-w.; Wang, H.-r.; Qiu, Z.-g.; Shen, Z.-q.; Shi, D.-y.; Li, H.-b.; Guo, J.-h.; Li, J.-w. Chlorine disinfection promotes the exchange of antibiotic resistance genes across bacterial genera by natural transformation. *ISME J.* **2020**, *14*, 1847−1856.
(45) Wang, Y.; Lu, J.; Engelstädter, J.; Zhang, S.; Ding, P.; Mao, L.; Yuan, Z.; Bond, P. L.; Guo, J. Non-antibiotic pharmaceuticals enhance the transmission of exogenous antibiotic resistance genes through bacterial transformation. *ISME J* **2020**, *14*, 2179−2196.
(46) Zhang, Y.; Gu, A. Z.; He, M.; Li, D.; Chen, J. Subinhibitory concentrations of disinfectants promote the horizontal transfer of multidrug resistance genes within and across genera. *Environ. Sci. Technol.* **2017**, *51*, 570−580.
(47) Dong, S.; Masalha, N.; Plewa, M. J.; Nguyen, T. H. Toxicity of wastewater with elevated bromide and iodide after chlorination, chloramination, or ozonation disinfection. *Environ. Sci. Technol.* **2017**, *51*, 9297−9304.